

Retention loss phenomena in hydrothermally fabricated heteroepitaxial PbTiO₃ films studied by scanning probe microscopy

W. S. Ahn, W. W. Jung, and S. K. Choi^{a)}

Department of Materials Science and Engineering, Korea Advanced Institute of Science and Technology, 373-1 Guseong-Dong, Yuseong-Gu, Daejeon 305-701, Republic of Korea

Yasuo Cho

Research Institute of Electrical Communication, Tohoku University, 2-1-1 Katahira, Aoba-ku, Sendai 980-8577, Japan

(Received 5 May 2005; accepted 26 January 2006; published online 21 February 2006)

We observed the retention loss phenomena of the nanodomains with an average diameter of 36 nm and that of the square domains with a size of 1 and 25 μm^2 that were reversed by an applying electric field at an atomic force microscopy conductive tip in a heteroepitaxial PbTiO₃ thin film, which was fabricated via hydrothermal epitaxy below Curie temperature, T_C . While the nanodomains did not undergo significant retention loss until 5.3×10^6 s, the square domains revealed some retention loss for a fixed period after long latent periods. The observed phenomena were explained in terms of the instability of the curved c/c domain wall and the compressive strain energy. Analyses showed that the nanodomains composed a cylinder extending to the bottom electrode; however, the square domains had a curved c/c domain wall, including the compressive strain energy, and these factors caused the retention loss. © 2006 American Institute of Physics. [DOI: 10.1063/1.2178417]

Recently, there has been considerable interest in ferroelectric films as a medium for nonvolatile memory devices.^{1,2} With ferroelectric materials, it is possible to control a spontaneous polarization direction corresponding to a data bit by applying an external electric field. In addition, the domain wall thickness of a typical ferroelectric material is only a few lattices (≤ 1 nm).³ In particular, much attention has been paid to investigating ultrahigh-density (over 1 Tbit/in.²) data storage using scanning probe techniques, such as scanning probe microscope-based ferroelectric data storage.^{4,5} The general requirements of nonvolatile data storage media are fast operating times, small bit size, and reliability related to long-term data retention and fatigue. However, most of the studies on domain switching behavior have focused on domain size and stability in relation to writing time and writing voltage.^{6,7} There have been few studies related to retention loss, which is defined as a decrease in a reversed domain size with time by the lateral movement of the c/c domain wall in the absence of an external field. Thus far, studies on such retention loss have been confined to polycrystalline films or 90° twinned domain structured films.⁸⁻¹¹ It was reported that the retention loss in polycrystalline PbZr_{1-x}Ti_xO₃ (PZT) films nucleates at the grain boundaries.^{8,9} Once the retention loss begins, it proceeds via lateral expansion of the back reversed portion. Also, for a PZT thin film with 90° twinned domain structure, the retention loss nucleates primarily at the twin domain boundaries and progresses inward.^{10,11} However, polycrystalline or twinned domain structured ferroelectric films are not useful for a data storage media application because both the grain and twin boundaries act as defects that inhibit polarization switching.

Hydrothermal epitaxy is a technique that utilizes aqueous chemical reactions to synthesize inorganic materials in

the form of epitaxial films on structurally similar single-crystal substrates under elevated pressure (below 15 MPa) and at low temperature.¹²⁻¹⁴ Recently, we fabricated a heteroepitaxial PbTiO₃ (PTO) film on a cubic Nb-doped (100) SrTiO₃ (NSTO) single crystal substrate by hydrothermal epitaxy under a hydrostatic pressure (compressive and below 15 MPa) at a temperature (160 °C) below T_C without including phase transition.¹⁵ A polarization versus electric field hysteresis loop with a remanent polarization of about 72 $\mu\text{C}/\text{cm}^2$ was clearly observed from our epitaxial PTO film on a cubic (100) NSTO single crystal substrate. In addition, examination with piezoresponse force microscopy (PFM) revealed that heteroepitaxial PTO film has a switchable $+c$ monodomain (upward polarization) at the as-fabricated state. In this study, nanodomains with an average diameter of 36 nm and square domains with sizes of 1 and 25 μm^2 were reversed using an atomic force microscopy (AFM) conductive tip on a heteroepitaxial PTO film with a $+c$ monodomain fabricated via hydrothermal epitaxy below Curie temperature; subsequently, the retention loss behaviors were examined. We will discuss the retention loss behaviors of the nanodomains and the square domains in terms of mechanical strain energy and c/c domain wall instability.

Heteroepitaxial PTO film with $+c$ monodomain was fabricated at 160 °C via hydrothermal epitaxy on a cubic (100) NSTO single crystal, which was each used as both a substrate and an n -type semiconductor bottom electrode. The PTO film had a thickness of ~ 200 nm. Details of the fabrication processes are provided in the relevant literature.¹⁵ The nanodomain array with an average diameter of 36 nm was reversed by -15 V on the bottom electrode with a pulse width of 2 ms using an AFM conductive tip with a tip radius of ~ 10 nm and a force constant of ~ 0.2 N/m.^{8,16} The square domains, with sizes of 1 and 25 μm^2 on PTO film, were reversed by scanning the conductive tip with a scanning speed of 2×10^{-6} m/s with -15 V on the bottom electrode.¹⁷

^{a)}Electronic mail: sikchoi50@kaist.ac.kr

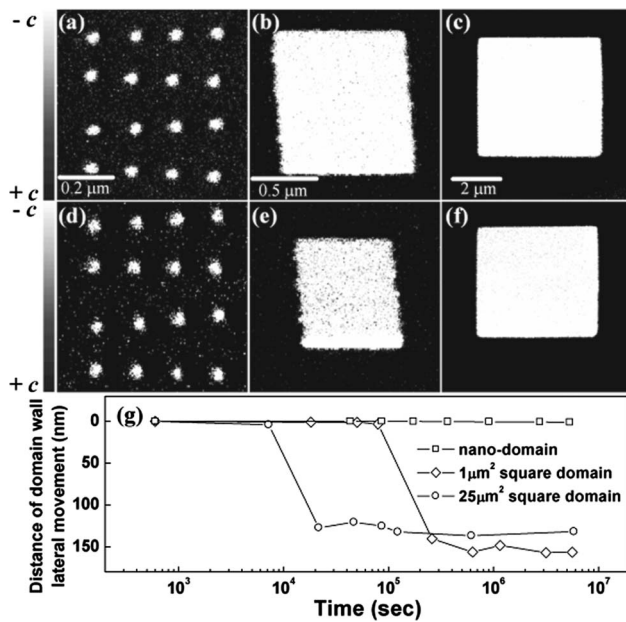


FIG. 1. PFM images of (a) the nanodomains, (b) 1 and (c) 25 μm^2 square domain in the PbTiO_3 thin film, which were taken immediately after domain reversal. (b), (d), and (f) show PFM images of the respective domains after 5.3×10^6 s, 5.6×10^6 s, and 5.8×10^6 s. (g) The distance of the lateral movement of the c/c domain wall plotted as a function of time for the nano-domain and the square domains in PbTiO_3 thin film.

The line step and direction of scanning were 256 and from left to right, respectively. In a previous study, a coercive field of PTO film was ~ 105 kV/cm.¹⁵ Therefore, it was assumed that the $-c$ domains (down polarization) reversed by -15 V were fully extended to the interface between the film and the bottom electrode, because an applied voltage of -15 V is approximately seven times higher than the coercive voltage. The retention loss was observed via a PFM (a commercial Seiko SPA 400) image. During the imaging, the film was scanned with an oscillating tip bias of 5 V_{pp} (peak to peak) at 8 kHz to the bottom electrode.

Figures 1(a)–1(c) show the PFM image of the nanodomains, the $1 \mu\text{m}^2$ square domain, and the $25 \mu\text{m}^2$ square domain reversed from the original $+c$ monodomain, respectively. These images were taken immediately after domain reversal. Figures 1(d)–1(f) show the PFM images of the respective domains after 5.3×10^6 s, 5.6×10^6 s, and 5.8×10^6 s. Figure 1(g) shows the quantitative representations of the observed retention loss, i.e., the distance of the lateral movement of the c/c domain wall. It can be seen from the figure that the nanodomains did not show significant retention loss until 5.3×10^6 s. In contrast, the c/c domain walls of the square domains clearly moved laterally for a fixed period after a latent period of $\sim 7.2 \times 10^3$ s ($25 \mu\text{m}^2$) and $\sim 8.0 \times 10^4$ s ($1 \mu\text{m}^2$). The retention loss in the square domains appears to be preceded only by the lateral movement of the c/c domain wall without nucleation of the opposite polarization in the inner part of the square domain.

Our heteroepitaxial PTO film has an only $+c$ monodomain at the virgin state. It is expected that the $-c$ domain, which is reversed by applying an external electric field, is more stable [state 1 of Fig. 2(a)], because the depolarization field is completely screened by the negative charges of the n -type semiconductor electrode at the interface.^{18,19} The origin of the $+c$ monodomain in our heteroepitaxial PTO film at

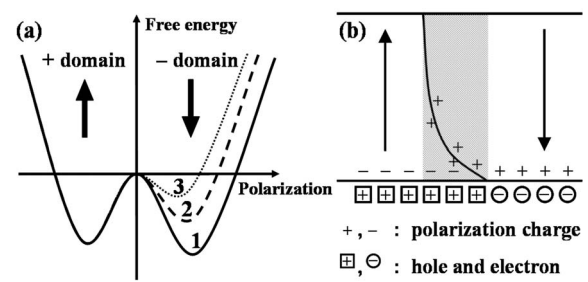


FIG. 2. (a) Schematic free energy diagrams of the $-c$ domain within the volume including the curved c/c domain wall. The each curve indicates the energy states of $-c$ domain (1) screened completely, (2) with the depolarization field energy, and (3) with the depolarization field energy and the compressive strain energy. (b) Schematic representation of the origin of the lateral movement of the c/c domain wall. Note that this figure shows only a half part of the cross-sectional domain structure.

the virgin state is not yet clear.¹⁵ If the $+c$ domain at the virgin state is reversed to the $-c$ domain by applying an external electric field, then the reversed $-c$ domain will be more stable. Therefore, it is expected that retention loss, i.e., the lateral movement of the c/c domain wall in our heteroepitaxial PTO film, cannot occur. However, for the square domains, the c/c domain wall moves laterally toward the center of the reversed $-c$ domain after latent periods. Thus, questions arise as to what causes the driving force for the lateral movement of the c/c domain wall in the absence of an external electric field, and as to why the nanodomain is stable.

When an external electric field is applied via the AFM tip, the electric field distribution in a film is inhomogeneous.^{20,21} Therefore, we assumed that the reversed domains had not straight but curved c/c domain wall, and extend to the bottom electrode as shown in Fig. 2(b). The head-to-head polarization structure, i.e., uncompensated positive charges, exists along the curved c/c domain wall. There are depolarization fields with an up direction, and these fields change with varying film thickness. We assumed that this depolarization fields are not compensated by free charges that exist intrinsically in the PTO film, because our film has a large remanent polarization and is not leaky.¹⁵ The electrostatic energy caused by the depolarization fields makes the curved c/c domain wall energy higher than the straight c/c domain wall energy (the domain wall instability). The free energy of the $-c$ domain within the volume, including the curved c/c domain wall [the shaded area in Fig. 2(b)], will increase more than that of the original $+c$ domain, as shown in state 2 of Fig. 2(a). It is thus possible that the domain wall instability contributes to the driving force for the $-c$ domain reversal, i.e., the lateral movement of the c/c domain wall toward the center of the $-c$ domain. Since the nanodomain has two-dimensional curvatures, compared to the square domain, the magnitude of the domain wall instability per unit volume within the shaded area shown in Fig. 2(b) should be larger than that on the square domain. Nevertheless, the retention loss phenomenon on the nanodomains was not observed. It appears, therefore, that the problem of the domain wall instability due to the depolarization field, i.e., the curved c/c domain wall is not involved in the nanodomains.

Figure 3 shows topography and line profiles of a $1 \mu\text{m}^2$ square domain in a PTO thin film before and after the domain reversal. The square domain clearly shrank toward the

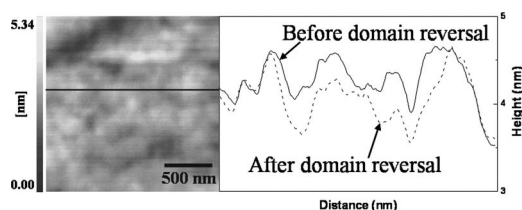


FIG. 3. Topography of $1 \mu\text{m}^2$ square domain in the PbTiO_3 thin film after the domain reversal. The right profiles show the line profiles before and after the domain reversal.

bottom electrode by ~ 1 nm after its reversal. The reversed $-c$ domain is in a compressive stress. The further increase of the free energy of the shaded area shown in Fig. 2(b) is caused by the compressive strain energy [state 3 of Fig. 2(a)].

As mentioned earlier, the latent periods for the lateral movement of the c/c domain wall are very long. We believe that these long latent periods indicate that the lateral movement of the c/c domain wall of the square domain is a thermally activated process for overcoming the energy barrier. Molotskii *et al.* reported that the domain wall movement is slowed down sharply and becomes thermally activated when the applied electric field is lower than the coercive field.²² We have confirmed experimentally that there was almost no the latent period for the lateral movement of the c/c domain wall of the square domain at the elevated temperature. The $+c$ domain nucleates in a point of maximal divergence of the polarization vector, because the depolarization field is highest in this point. After the nucleation, the $+c$ domain grows toward the film surface, resulting in the lateral movement of the c/c domain wall. It is reasonable to think that the compressive strain energy increases with an expansion of the reversed domain size. Therefore, the latent period of the $25 \mu\text{m}^2$ domain for the lateral movement of the curved c/c domain wall is shorter than that of $1 \mu\text{m}^2$ domain. As shown in Fig. 1(g), it appears that the lateral movement of the c/c domain wall does not progress any longer after specific retention loss. Therefore, we expected that the lateral movement of the c/c domain wall stopped because the curved c/c domain wall became straight wall. During this situation, the whole $-c$ domain is energetically more stable even though it is in a compressive stress. Another possible phenomenon of the lateral movement of the c/c domain wall of the square domains is the $+c$ domain reversal within the shaded area shown in Fig. 2(b). Unfortunately, this phenomenon cannot be observed experimentally in all cases. From our experimental results, it is possible that, if the c/c domain wall parallel to c axis is created during the domain reversal process, the lateral movement of the straight c/c domain wall does not occur in the absence of an external electric field. We confirmed this phenomenon by poling our heteroepitaxial PTO film capacitor with a Ni top electrode of $50 \mu\text{m}^2$ size. We expected that the $-c$ domain with the c/c domain wall parallel to the c axis would be created by this process. In this case, lateral movement of the c/c domain wall was not observed.

Li *et al.* reported that the cylindrical domains extending to bottom electrode and having radius over 3 nm were stable.²³ Therefore, the nanodomains in this study had nearly a straight c/c domain wall, i.e., cylindrical domains because they did not show almost retention loss. It appears that the

domain reversal conditions (-15 V, a pulse width of 2 ms, and 200 nm film thickness) for the nanodomains are sufficient to form the cylindrical domains extending to the bottom electrode, as discussed by Emelyanov.²¹ However, the square domains were reversed by scanning the conductive-tip with a scanning speed of 2×10^{-6} m/s with -15 V on the bottom electrode. It is expected that this condition is not suitable for a straight c/c domain wall, even if more experimental study need to be performed.

In summary, we observed the retention loss of nanodomains (36 nm diameter) and square domains with sizes of 1 and $25 \mu\text{m}^2$ that were reversed by applying an electric field at a conductive AFM tip in a heteroepitaxial PbTiO_3 thin film, which was fabricated via hydrothermal epitaxy below T_C . While the nanodomains did not undergo significant retention loss, the square domains revealed retention loss phenomena. These observed phenomena have been explained in terms of the instability of the curved c/c domain wall and the compressive strain energy. Analyses have shown that the nanodomains composed a cylinder extending to the bottom electrode; however, the square domains had a curved c/c domain wall, including the compressive strain energy, and these factors caused the retention loss.

This work was supported by the Korean Ministry of Science and Technology (M1010500066-01H2006400), the National Research Laboratory Program (M10400000024-04J0000-02410), and the Brain Korea 21 project of 2005.

¹J. F. Scott and C. A. Araujo, *Science* **246**, 1400 (1989).

²C. A. Paz de Araujo, J. D. Cuchiaro, L. D. McMillan, M. C. Scott, and J. F. Scott, *Nature (London)* **374**, 627 (1995).

³F. Jona and G. Shirane, *Ferroelectric Crystals* (Pergamon, Oxford, 1962), p. 46.

⁴T. Hidaka, T. Mayurama, M. Saitoh, N. Mikoshiba, M. Shimizu, T. Shiosaki, L. A. Wills, R. Hiskes, S. A. Dicarolis, and J. Amano, *Appl. Phys. Lett.* **68**, 2358 (1996).

⁵C. H. Ahn, T. Tybell, L. Antognazza, K. Char, R. H. Hammond, M. R. Beasley, Ø. Fisher, and J.-M. Triscone, *Science* **276**, 1100 (1997).

⁶P. Paruch, T. Tybell, and J.-M. Triscone, *Appl. Phys. Lett.* **79**, 530 (2001).

⁷Y. Cho, K. Fujimoto, Y. Hiranaga, Y. Wagatsuma, A. Onoe, K. Terabe, and K. Kitamura, *Nanotechnology* **14**, 637 (2003).

⁸A. Gruverman, H. Tokumoto, A. S. Prakash, S. Aggarwal, B. Yang, M. Wuttig, R. Ramesh, O. Auciello, and T. Venkatesan, *Appl. Phys. Lett.* **71**, 3492 (1997).

⁹D. Fu, K. Suzuki, K. Kato, M. Minakata, and H. Suzuki, *Jpn. J. Appl. Phys., Part 1* **41**, 6724 (2002).

¹⁰C. S. Ganpule, V. Nagarajan, S. B. Ogale, A. L. Roytburd, E. D. Williams, and R. Ramesh, *Appl. Phys. Lett.* **77**, 3275 (2000).

¹¹C. S. Ganpule, A. L. Roytburd, V. Nagarajan, B. K. Hill, S. B. Ogale, E. D. Williams, R. Ramesh, and J. F. Scott, *Phys. Rev. B* **65**, 014101 (2001).

¹²F. F. Lange, *Science* **273**, 903 (1996).

¹³A. T. Chien, J. Sachleben, J. H. Kim, J. S. Speck, and F. F. Lange, *J. Mater. Res.* **14**, 3303 (1999).

¹⁴A. T. Chien, X. Xu, J. H. Kim, J. Sachleben, J. S. Speck, and F. F. Lange, *J. Mater. Res.* **14**, 3330 (1999).

¹⁵W. W. Jung, H. C. Lee, W. S. Ahn, S. H. Ahn, and S. K. Choi, *Appl. Phys. Lett.* **86**, 252901 (2005).

¹⁶L. M. Eng, *Nanotechnology* **10**, 405 (1999).

¹⁷A. Gruverman, O. Auciello, R. Ramesh, and H. Tokumoto, *Nanotechnology* **8**, A38 (1997).

¹⁸P. Wurfel and I. P. Batra, *Phys. Rev. B* **8**, 5126 (1973).

¹⁹P. Wurfel, I. P. Batra, and J. T. Jacobs, *Phys. Rev. Lett.* **23**, 1218 (1973).

²⁰M. Molotskii, *J. Appl. Phys.* **93**, 6234 (2003).

²¹A. Y. Emelyanov, *Phys. Rev. B* **71**, 132102 (2005).

²²M. Molotskii, A. Agronin, P. Urenski, M. Shvbelman, G. Rosenman, and Y. Rosenwaks, *Phys. Rev. Lett.* **90**, 107601 (2003).

²³X. Li, A. Mamchik, and I.-W. Chen, *Appl. Phys. Lett.* **79**, 809 (2001).